Active and reactive power control of the doubly fed induction generator based on wind energy conversion system

CrossMark

Ghulam Sarwar Kaloi [a,*], Jie Wang [a,*], Mazhar Hussain Baloch [a,b]

[a] *School of Electronic Information and Electrical Engineering, Shanghai Jiao Tong University, PR China*
[b] *Department of Electrical Engineering, MUET, SZAB Khairpur Mir's Campus Pakistan, Pakistan*

ABSTRACT

This paper presents a dynamic modeling and control of doubly fed induction-generator (DFIG) based on the wind turbine systems. Active and reactive power control of the DFIG are based on the feedback technique by using the suitable voltage vectors on the rotor side. The rotor flux has no impact on the changes of the stator active and reactive power. The proposed controller is based on the feedback technique in order to reduce the oscillation of the generator. The control approach is estimated through the simulation result of the feedback controller assembled with DFIG wind turbines. It is applied by the feedback control based techniques in order to control the power flowing of DFIG and the power grid. Hence, an improved feedback control technique is adopted to get a better power flow transfer and to improve the dynamic system and transient stability. In stable condition, the improved performance of the controller, the proposed method is verified for the effectiveness of the control method is done in stable conditions.

© 2016 The Authors. Published by Elsevier Ltd.
This is an open access article under the CC BY-NC-ND license
(http://creativecommons.org/licenses/by-nc-nd/4.0/).

1. Introduction

The renewable energy resources have emerged as a new model to meet the energy requirements of our society. In recent years, the production of electricity from hydropower, solar, the wind and geothermal energy, tides, waves and biomass energy sources have gained much attention (Yaramasu et al., 2015). Energy is considered to be the decisive input for the growth of the wind energy. Nowadays, conventional resource depletion is more concerned about environmental degradation and takes advantage of renewable energy resources to meet growing energy demands. Energy production cost is very low as compared to the conventional method. The potential sources of clean energy are considered for the future such as wind energy. For electricity production through wind energy, DFIG is commonly used for this purpose because of its numerous advantages over its counterparts (Dinesh and Rajasekaran, 2015; Ebrahimi et al., 2016).

Variable speed operation of the DFIG wind turbine based on the active and reactive power abilities, lower cost of the converter and power losses are decreased as compared to wind turbine by using the fixed speed generator. Variable speed wind turbines with the new standards are effective because of their improved efficiency in capturing more wind power and their ability to achieve the higher power quality (Luna et al., 2011; Tohidi and Behnam, 2016).

Moreover, wind turbine of the variable speed with control of the speed of the turbine output power and reduces the load stress on different parts of the turbine structure, including the blades and tower. As a result, higher energy efficiency, longer life time, and improve the quality of energy to make these wind turbines inexpensively competitive, despite the high initial costs (Zhan et al., 2014; Baloch et al., 2016; Yang et al., 2012). The dynamic model of DFIG depends upon the non-linear parameters such as electromagnetic torque, stator current; rotor current and stator flux are controlled with state feedback linearization techniques to get the better results as compared to the exit method (Baroudi et al., 2007; Hu et al., 2010). Implementation of DFIG is increasing for many reasons, such as reducing the mechanical stress, to mitigate the noise, and flexible control of the active and reactive power on the basis of back to back converter between the induction machine and the power grid (Mishra et al., 2009; Rahimi, 2016).

As a result, the complexity of the system increases and it becomes difficult to analyze without a systematic point of view. In short terms, there must be the ability to support dynamic frequency of wind energy rapidly in the near future to ensure the stability of the frequency of the system. In addition, it can be

---

* Corresponding authors.
   E-mail addresses: ghulamsarwar@sjtu.edu.cn (G.S. Kaloi),
jiewangxh@sjtu.edu.cn (J. Wang).

contributed to the inertia of wind energy to further improve the accessibility of wind power in the grid (Zhan et al., 2014; Xiao et al., 2013; Hu et al., 2010). In order to control the generator speed is used to rotor side converter (RSC) and reactive power controlled with grid side converter (GSC) is connected to the grid through grid filter and is used to control the dc link voltage and reactive power exchange with the grid.

Hence with increased penetration of the DFIG, the inertia of the effective system will be reduced. Grid integration of this variable power in increased capacity raises concerns about its impact on the power system stability (Carrasco et al., 2006; Gayen et al., 2015). Nonetheless, it is imperative for large scale transient strength studies to consider the rotor field elements of the induction generator since it assumes a critical part in deciding the inner voltage behind transient reactance. In order to reduce the efficiency of the machine due to the response of reactive power is increased. But state feedback linearization control technique is used to improve the efficiency of the machine and reduce the transient effect in the system. (Yousefi-Talouki et al., 2014; Abdel-Khalik et al., 2013).

This paper proposes a new strategy for feedback control systems for wind power generation on the basis of DFIG with constant switching frequency to improve transient performance. The direct method in calculating the required voltage circuit control the transition period, based on the estimated stator flux, active and reactive power, and their errors. The transient performance of the nonlinear model of the DFIG is described by the limit of the rotor control voltage with a direct method of the active and reactive power. The aim of this paper is to provide a great idea for the dynamic behavior of the DFIG wind turbine. Control of DFIG parameters has a significant effect on the dynamic performance of wind turbines. The controller of the DFIG will play an important role in the energy system in the future with the increased penetration of the wind energy conversion system (WECS) (Bourdoulis and Alexandridis, 2014; Wang and Wang, 2011).

The proposed technique is considered by the feedback controller to regulate the rotor currents and the grid current. In order to consider the effects of the rotor and the filter of network parameters to control the dynamic performance DFIG under voltage dips. It represents the vital phenomena that are much faster than the phenomena of interest in transient stability analysis. The use of the detailed model in the study of transient stability leads to a harsh mathematical model with fast transients and long simulation times and greatly increases the computational effort. In any case, as a result of complexity of the DFIG model, extra suppositions are utilized as a part of the transient stability program for simplifying it (Naidu et al., 2014; Trilla et al., 2014). In this paper, feedback control design is developed and considered for the DFIG wind turbine system. Non-linear dynamic model of the DFIG is essentially based on stator flux as compared to conventional flux model of the wound rotor induction generator and GSC model. Non-linear dynamic model of the DFIG is improved by using the feedback control technique for alignment of the rotor and grid sides. Active and reactive power of the DFIG stator and GSC output are connected to the grid. This paper is organized as follows: in Section 2 wind turbine model is described. In Section 3 dynamic model of the DFIG wind energy System is developed. In Section 4, a controller is designed for a DFIG Wind Turbine System. The simulation results are shown in Section 5. Final conclusion of the paper is described in Section 6.

2. Wind turbine model

The captured mechanical power from a wind turbine is given as follows (Yang et al., 2012):

$$P_m = 0.5 \rho A V_\omega^3 C_p(\lambda, \beta), \tag{1}$$

where ρ represents the air density, R_T represents the wind turbine radius, V_w represents the wind speed and C_p represents the wind turbine power coefficient is given by

$$C_p(\lambda, \beta) = 22 \left(\frac{1.16}{\lambda_i} - 0.004\beta - 0.05 \right) e^{-12.5\frac{1}{\lambda_i}}, \tag{2}$$

$$\frac{1}{\lambda_i} = \frac{1}{\lambda + 0.08\beta} - \frac{0.035}{\beta^3 + 1}, \tag{3}$$

where β represents the blade pitch angle and λ represents the tip speed ratio as described below.

$$\lambda = \frac{\omega_r R_T}{V_w}. \tag{4}$$

Owing to the presence of a gearbox with the gear ratio n_g, the dynamic model wind turbine rotational speed ω_r is associated to the rotor speed ω_r is given as follows:

$$\omega_r = n_g \omega_r^{optimum}. \tag{5}$$

The exact dynamic model of the torque equation of the generator is given by,

$$T_m \omega_r = P_m \tag{6}$$

where, T_m represents the rotor torque, ω_r represents the wind turbine speed, it is a measure of the ratio of wind power turbines. Power coefficient is a function of wind turbine speed. C_p is 0.59 the theoretical limit, but practical range is 0.2–0.4 (Patel, 2005).

$$\omega_r^{optimum} = \frac{1}{R_T} \lambda_{optimum} n_g V_w. \tag{7}$$

Which corresponds to the most extreme extraction of wind energy $P_m^{\max}$, at that point in the determination of the rotor torque of the generator can be determined as

$$T_m^{optimum} = 0.5 \rho \pi R_T^5 C_p^{optimum} \omega_r^{optimum} \left(\lambda_{optimum}^3 \right)^{-1}. \tag{8}$$

It is obvious that the wind turbine operates with ideal rotational speed and with the optimum torque of the doubly fed induction generator.

3. Dynamic model of the DFIG wind energy system

The power convertor of the wind turbine generator contains the rotor converter to control the generator speed and grid convertor to inject reactive power in the grid. The grid side converter components of the real and reactive power are shown in Fig. 1. The instantaneous power can be defined as follows (Krause et al., 2013):

$$P_s = 1.5(V_{ds}I_{ds} + V_{qs}I_{qs}); \tag{9}$$

$$Q_s = 1.5(V_{qs}I_{ds} - V_{ds}I_{qs}), \tag{10}$$

$$P_g = 1.5(V_{ds}I_{dg} + V_{qs}I_{qg}) \tag{11}$$

$$Q_g = 1.5(V_{qs}I_{dg} - V_{ds}I_{qg}) \tag{12}$$

where P_s and Q_s represent the active and reactive power stator of the DFIG respectively, and P_g and Q_g represent the active and reactive power of the grid respectively. The nonlinear dynamic model of the DFIG wind turbine is normally described by the active and reactive powers. To simplify the dynamic model is assuming an approximately constant stator voltage for DFIG. This assumption is used only under a steady state condition and grid voltages vary at the point of the common coupling typically less than ±0.005 p.u.
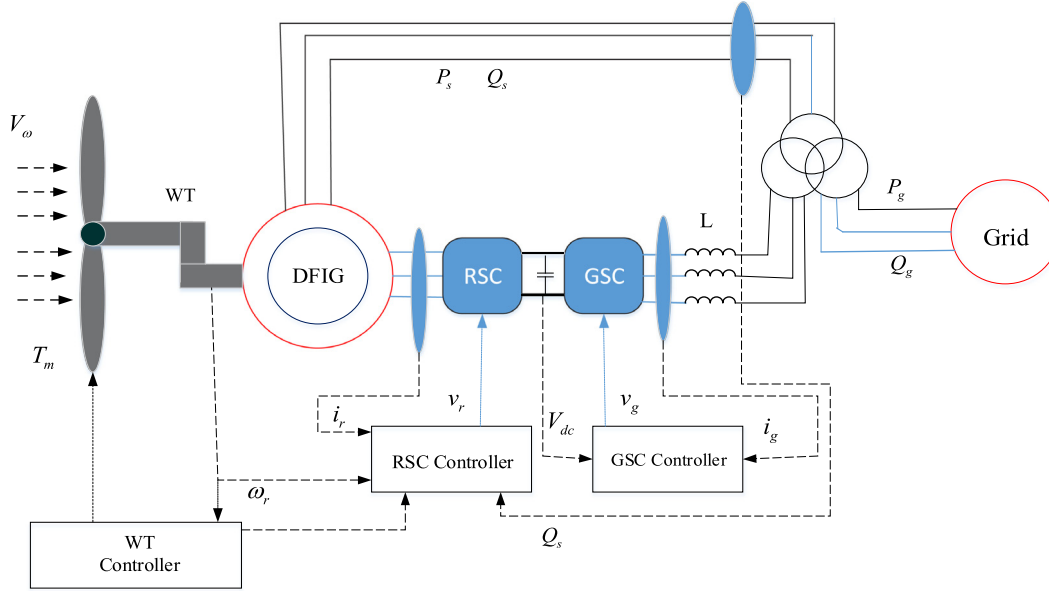
Fig. 1. Schematic diagram of wind energy based on DFIG system.

3.1. The DFIG wind turbine system modeling in the dq reference frame

The nonlinear dynamic model of the doubly fed induction generator represents the flux and the voltage equations can be summarized as (Rezaei et al., 2012):

$$\frac{d}{dt}\lambda_{ds} = V_{ds} - r_s I_{ds} + \omega_s \lambda_{qs} \tag{13}$$

$$\frac{d}{dt}\lambda_{qs} = V_{qs} - r_s I_{qs} - \omega_s \lambda_{ds} \tag{14}$$

$$\frac{d}{dt}\lambda_{dr} = V_{dr} - r_r I_s + (\omega_s - p\omega_r)\lambda_{qr}, \tag{15}$$

$$\frac{d}{dt}\lambda_{qr} = V_{qr} - r_r I_s - (\omega_s - p\omega_r)\lambda_{dr} \tag{16}$$

and

$$\lambda_{ds} = l_s I_{ds} + l_m I_{dr}; \qquad \lambda_{dr} = l_r I_{dr} + l_m I_{ds} \tag{17}$$

$$\lambda_{qs} = l_s I_{qs} + l_m I_{qr}. \qquad \lambda_{qr} = l_r I_{qr} + l_m I_{qs} \tag{18}$$

where, R_s and R_r are the stator and rotor resistance, l_s and l_r are the stator and rotor inductance while l_m represents the mutual inductance, ω_s is the synchronous (stator) frequency respectively. Subscript S and r indicates the stator and rotor variables. In addition V_s, I_s and λ_s represent the stator voltage, current and stator flux, V_r, I_r and λ_r are represent the rotor voltages, current and flux vectors.

By substituting Eqs. (17) and (18) into Eqs. (13) and (14) for $\frac{d}{dt}I_{ds}$ and $\frac{d}{dt}I_{qs}$, the following equation can be obtained:

$$\frac{d}{dt}I_{ds} = -\frac{r_s}{\sigma l_s}I_{ds} + \omega_s I_{qs} + r_r\frac{l_m}{\sigma l_s l_r}I_{dr} + \frac{p\omega_r l_m}{\sigma l_s}I_{qr}$$
$$+ p\frac{l_m^2 \omega_r}{\sigma l_s l_r}I_{qr} - \frac{l_m}{\sigma l_s l_r}V_{dr} + \frac{V_{ds}}{\sigma l_s}, \tag{19a}$$

$$\frac{d}{dt}I_{qs} = \omega_s I_{ds} - \frac{r_s}{\sigma l_s}I_{qs} + \frac{p\omega_r l_m}{\sigma l_s}I_{dr} + r_r\frac{l_m}{\sigma l_s l_r}I_{qr}$$
$$+ p\frac{l_m^2 \omega_r}{\sigma l_s l_r}I_{ds} - \frac{l_m}{\sigma l_s l_r}V_{qr} + \frac{V_{qs}}{\sigma l_s}, \tag{19b}$$

where,

$$\sigma = (l_r l_s - l_m^2)/(l_r l_s).$$

Using Eqs. (9) and (10) into Eqs. (19a) and (19b) the following equation can be obtained.

$$\frac{d}{dt}P_s = -\frac{2}{3}\alpha_1(r_s l_r + r_r l_s)P_s - \omega_{slip}Q_s$$
$$+ (\alpha_1 r_r V_{ds} + p\alpha 1 l_r V_{ds}\omega_r)\lambda_{ds}$$
$$+ (\alpha_1 r_r V_{qs} + p\alpha 1 l_r V_{qs}\omega_r)\lambda_{qs}$$
$$- \alpha_1 l_m V_{ds}V_{dr} + \overline{V}_{qr} \tag{20a}$$

$$\frac{d}{dt}Q_s = \omega_{slip}P_s + \frac{2}{3}\alpha_1(r_s l_r + r_r l_s)Q_s$$
$$+ (\alpha_1 r_r V_{qs} + p\alpha 1 l_r V_{qs}\omega_r)\lambda_{qs}$$
$$+ (\alpha_1 r_r V_{ds} + p\alpha 1 l_r V_{ds}\omega_r)\lambda_{ds}$$
$$- \alpha_1 l_m V_{ds}V_{dr} + \alpha_1 l_m V_{ds}V_{qr} \tag{20b}$$

where,

$$\alpha_1 = \frac{3}{2\sigma l_r l_s}, \qquad \overline{V}_{qr} = \alpha_1 l_m V_{qs}V_{qr} + \alpha_1 l_r V_s^2.$$

The equation of the stator flux can be described by substituting for I_s from (12) into (13) for $\dot{\lambda}_{sd}$ and $\dot{\lambda}_{sq}$

$$\frac{d}{dt}\lambda_{ds} = \alpha_3 r_r V_{ds}P_s - \alpha_3 r_r V_{qs}Q_s + \omega_s \lambda_{qs}, \tag{21a}$$

$$\frac{d}{dt}\lambda_{qs} = -\alpha_3 r_r V_{qs}P_s + \alpha_3 r_r V_{ds}Q_s + \omega_s \lambda_{ds} \tag{21b}$$

where, $\alpha_3 = \frac{2r_s}{3r_r V_s^2}$.

The nonlinear dynamic model of the DFIG wind turbine equation of the rotor and torque model is given as follows (Balogun et al., 2013):

$$\frac{d}{dt}\omega_r = \frac{P}{J}T_e - \frac{P}{J}T_m, \tag{22}$$

where P, J and T_m are the number of pole pairs of the machine, rotor inertia and mechanical torque of the machine respectively.

The electric torque is given (see Krause et al., 2013):

$$T_e = 1.5p(\lambda_{qs}I_{dr} + \lambda_{ds}I_{qr}). \tag{23}$$

In Eq. (17) mechanical torque is the input of the dynamic model and electric torque based on Eq. (18). It can be expressed in terms
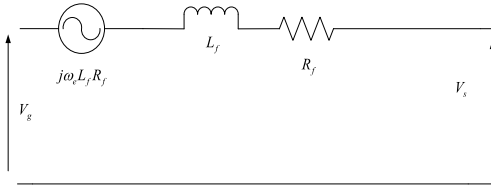
Fig. 2. Equivalent circuit of the grid side convertor.

of active and reactive power. By substituting (23) into (22), the following equation can be obtained:

$$\frac{d}{dt}\omega_r = -\frac{P^2}{JV_s}\lambda_{sq}P_s + \frac{P^2}{JV_s}\lambda_{sd}Q_s - \frac{P}{J}T_m. \tag{24}$$

3.2. Grid-side convertor and filter model

The grid sides filter convertor is shown in Fig. 2. The *dq* model of grid side convertor and the filter are given as follows (Lei et al., 2006):

$$l_fI_{df} = -r_fI_{df} + \omega_sl_fI_{qf} - V_{dg} + V_{ds} \tag{25}$$

$$l_fI_{qf} = -\omega_sl_fI_{df} - r_fI_{qf} - V_{qg} + V_{qs} \tag{26}$$

where, V_g represents the grid voltage, I_g represents the grid current, l_f represents the filter inductance and R_f represents the filter resistance. Substituting the Eqs. (24) and (25) into Eqs. (11) and (12) the following equation can be obtained.

$$\frac{d}{dt}P_g = -\frac{r_f}{l_f}P_g - \omega_sQ_g - 1.5\frac{V_{ds}}{l_f}V_{dg} - \overline{V}_{qg} \tag{27a}$$

$$\frac{d}{dt}Q_g = \omega_sP_g - \frac{r_f}{l_f}Q_g - 1.5\frac{V_{ds}}{l_f}V_{dg} + 1.5\frac{V_{ds}}{l_f}V_{qg}. \tag{27b}$$

Now we take equivalent real power of the dynamic model of the DFIG, which can be obtained in the DC link model at the DC converter node as follows (Wang and Wang, 2011):

$$V_{dc}(t)I_{dc}(t) = P_g(t) - P_r(t) - P_{loss}(t), \tag{28}$$

where $P_r(t)$ represents active power of the rotor, $P_g(t)$ represents the grid power and P_{loss} represents the power losses, including the converter switching losses and the copper losses. The active power P_r delivered to the rotor (Rezaei et al., 2012).

$$P_r = 1.5\left[V_{rd}I_{rd} + V_{rq}I_{rq}\right]. \tag{29}$$

Using Eqs. (9), (10) and (18) P_r can be expressed as

$$P_r = \frac{l_s(V_{ds}V_{rd} + V_{qs}V_{rq})}{l_m|V_s|^2}P_s + \frac{l_s(V_{qs}V_{rd} + V_{ds}V_{rq})}{l_m|V_s|^2}Q_s$$
$$+ 1.5\frac{\lambda_{ds}}{l_m}V_{rd} + 1.5\frac{\lambda_{qs}}{l_m}V_{rq}. \tag{30}$$

In the high power convertor, the power loss is often less than one percent of the total transferred power, power losses are neglected because they are very small.

$$\frac{d}{dt}V_{dc} = \frac{P_g - P_r}{CV_{dc}}. \tag{31}$$

Substituting Eq. (29) into Eq. (30) the following equation can be expressed as

$$\frac{d}{dt}V_{dc} = \frac{1}{CV_{dc}}\left\{[P_g] - \left[\frac{1}{l_m|V_s|^2}\langle l_s(V_{ds}V_{rd} + V_{qs}V_{rq})P_s \right.\right.$$
$$\left.\left. + l_s(V_{qs}V_{rd} + V_{ds}V_{rq})Q_s\rangle + 1.5\frac{\lambda_{ds}}{l_m}V_{rd} + 1.5\frac{\lambda_{qs}}{l_m}V_{rq}\right]\right\}. \tag{32}$$

4. Proposed controller design for a DFIG wind turbine generator

In this study, we proposed a controller through feedback algorithm for DFIG transient stability analysis of WECS in order to obtain accurate results and simulation on the basis of well-known tool Matlab. It is well known that the transient stability analysis under the typical situation which is dominated by conventional synchronous generators. In the proposed method, the most important intention is to reduce the voltage disturbance under normal operating conditions. The controller design technique is used to achieve the best outcome of the wind energy conversion system. The control method of DC voltage deals with the rotor voltage to control the suitable parameters of the DFIG, such as stator flux, stator current, active and reactive power of the machine. The control of the RSC is utilizing the controller for power flow from the DFIG as depicted in Fig. 3.

It is the most important intention to maintain the DC link voltage and an effect to deal with the active power transfer between the RSC and the grid. The DC link voltage is operated to the below rated value of the GSC. The proposed technique is used to eliminate the transient from the DFIG to improve the performance of the machine. The control technique is minimized by the reactive power in order to achieve the best outcomes from the dynamic system that can be used for RSC and GSC to reduce the dynamic transient from the system.

The proposed system state variables are given as follows:

$$x = \begin{bmatrix} P_s & Q_s & \lambda_{ds} & \lambda_{qs} & P_g & Q_g \end{bmatrix}^T. \tag{33}$$

The dynamic model of the doubly fed induction generator is given in the (19a)–(20b) and (32)–(34) and can be summarized as:

$$\dot{x} = Ax + B_1U_1 + B_2U_2 \tag{34}$$

where

$$A = \begin{bmatrix} A_{11} & A_{12} \\ A_{21} & A_{22} \end{bmatrix}, \qquad B_1 = \begin{bmatrix} B_{11} \\ B_{12} \end{bmatrix}, \qquad B_2 = \begin{bmatrix} B_{22} \\ B_{23} \end{bmatrix}$$

$$U_1 = \begin{bmatrix} \overline{V}_{dr} \\ V_{qr} \end{bmatrix}, \qquad U_2 = \begin{bmatrix} \overline{V}_{dg} \\ V_{qg} \end{bmatrix}.$$

Control of the real power is obtained by controlling the rotor current of the *dq* axis component. The rotor side converter is to improve the performance of DFIG, and the real power of the DFIG is controlled with rotor voltages to increase the efficiency of the machine. The target of the controller design procedure is to improve the performance of wind energy conversion while maintaining the stability of the system under normal operating conditions. In the conventional variable speed of the DFIG wind turbine, it is extracting maximum rated power from the turbines unless the rated speed lower than the wind turbine speed (Asl and Yoon, 2016). The feedback linearization techniques are typically controlled to the real power of DFIG wind turbine based on wind energy conversion based. When wind speed is below the rated value, the feedback linearization technique is maximized to capture the energy from the wind turbine. To produce the maximum possible power from the wind turbine is based on its average amount of wind speed (Junyent-Ferré et al., 2010). It is noted that a new design of technique for feedback control has been established which guarantees stability, and significant simplification. The controller has been implemented for the nonlinear dynamic model of the DFIG. The RSC and GSC are required only for voltage orientation due to simpler control design for DFIG.

The feedback control strategy is used for the stator voltage and current control of the DFIG wind turbine system. These input parameters V_{dr}, V_{qr}, $\overline{V}_{dg}$ and V_{qg} are used to control the stator

Table 1
1.5 MW DFIG wind turbine parameters.

Symbol	Quantity	Values	Symbol	Quantity	Values
R_s	Stator resistance	1.4 mΩ	R_f	Grid filter resistance	0.04 Ω
R_r	Rotor resistance	0.99 mΩ	l_f	Grid filter inductance	0.001 H
l_s	Stator inductance	0.08998 mH	R_L	Load resistance	4.16 Ω
l_r	Rotor inductance	0.08208 mH	l_L	Load inductance	4.093 H
l_m	Mutual inductance	1.526 mH	F	Frequency	50 Hz
P	Pole pairs	3	V_ω	Wind speed	12 m/s
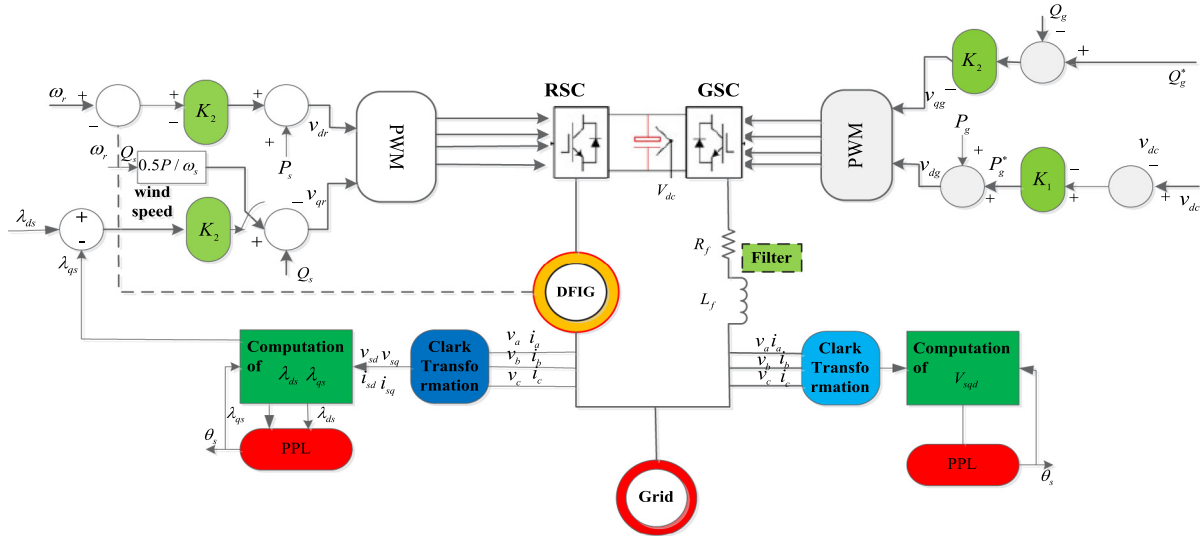
Fig. 3. Over all control diagram and study system of the nonlinear dynamic model of the DFIG.

real power and reactive power. The active and reactive power are controlled independently via V_{dr} and V_{qr}, respectively. The state feedback linearization control is achieved by controlling the reactive power to keep it within the desired range. The pulse width modulation is employed to generate the control signal V_r and V_g both are derived from the RSC and GSC. Overall system oscillation is decreased by using a control signal after the disturbance elimination. It is an easy way to use the voltage single V_r and V_g as input parameters of the controller. Under all circumstances, it is easy to measure the angular velocity and fluxes and it has been implemented in the steady state condition. The analysis of the DC link voltage is equivalent to the stable system under normal operating conditions of the wind turbine. We take the following enhanced model.

Again, we conclude (24) and (31) as follows:

$$\frac{d}{dt}\omega_r = x^T \tilde{C}x + \tilde{C}_o,$$ (35)

$$\frac{d}{dt}V_{dc}^2 = E_1 X + X E_3 U_1 + X E_2 U_1$$ (36)

where

$$\tilde{C} = \begin{bmatrix} 0_{2\times4} & 0_{2\times2} \\ 0_{2\times4} & c_{11} \\ 0_{2\times4} & 0_{2\times2} \end{bmatrix}, \qquad \tilde{C}_0 = \frac{P}{J}\begin{bmatrix} T_m \\ 0_{5\times1} \end{bmatrix},$$

$$E_1 = \begin{bmatrix} 1 \\ 0_{5\times1} \end{bmatrix}, \qquad E_3 = \begin{bmatrix} E_{11} \\ E_{21} \\ E_{31} \end{bmatrix},$$

$$E_2 = \begin{bmatrix} 0_{2\times2} \\ E_{22} \\ 0_{2\times2} \end{bmatrix}, \qquad E_2 = \begin{bmatrix} 0_{2\times2} \\ E_{22} \\ 0_{2\times2} \end{bmatrix}.$$

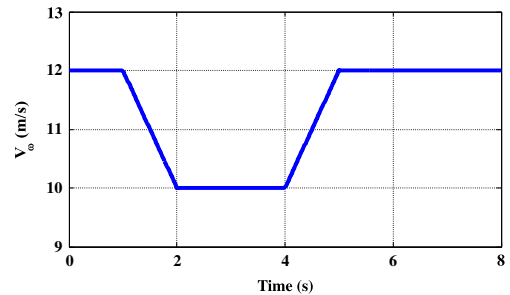**Fig. 4.** Wind speed versus time.

5. Simulation results and discussion

The analysis of proposed scheme and performance of the controller is extensively estimated in this section and by using real-time data to obtain the results. The 1.5-MW DFIG wind turbine parameters are presented in Table 1. The state of feedback linearization controller gains are given in the Appendix. However, in the simulation environment, we have verified the effectiveness of the proposed controller of DFIG wind turbine systems considering a case 1.5 MW, at 575 V_{rms} and at 50 Hz frequency. Moreover, the wind always vary from time to time due to uncertain wind conditions, we are considering a ramp change around in between 10 and 12 m/s and can be easily visualized in Fig. 4. The newly generated state variables of the controller are depicted as in Figs. 5–9. Therefore, our main focus is to control and to get maximum power at the grid side. The stator flux response versus time of the DFIG is depicted in Fig. 5, where it is observed that the exactly after 2.5 a very small change in the flux occurs. Furthermore, the rotor speed response has been discussed in Section 3 in Eq. (15), can be controlled around after 0.1 up as shown
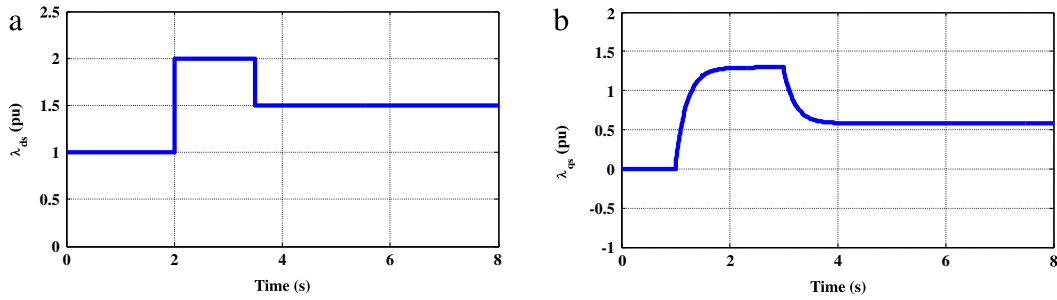
Fig. 5. (a) Response of the stator flux λ_{ds} versus time, (b) response of the stator flux λ_{qs} versus time.
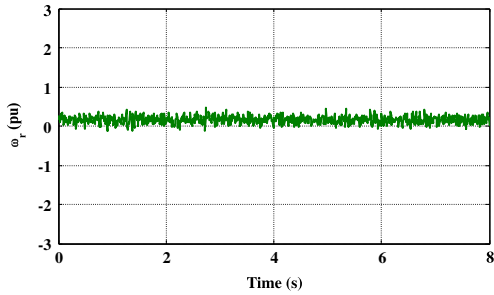

Fig. 6. Response of the angular rotor speed ω_r versus time.
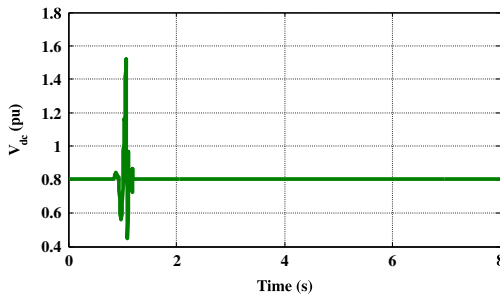

Fig. 7. Response of the DC voltage V_{dc} versus time.

in Fig. 6. Besides that, the voltage of a dynamic system is improved by the DC link around after 1.2 s on the both sides of the rotor and grid as showed in Fig. 7. As summarized in Eq. (23). Fig. 8 shows that the reactive and real power response versus time has a better performance of DFIG at 0.4 p.u after 1.1 s recover the fault or remove the disturbance and it can be observed to improve the stability and damping characteristics after the symmetrical fault. In order to validate the performance of the proposed controller with the conventional one, the real power varies with the small step change from 0.4 p.u to −0.6 p.u, and at the same time reactive power is set to be around zero (p.u). The real and reactive power time settlement is small and is without the overshooting of symmetrical fault as shown in Fig. 8. The proposed method easily tracks the reference signal of the real and reactive power of a dynamic system as showed in Fig. 9. It is verified that the proposed control method is robust in performance than the conventional method as described in Rezaei et al. (2012). In addition, it is clearly observed that the peak value of the DC-link voltage is minimized. Finally, DFIG wind turbine system performance is improved.

6. Conclusion and future work

The model has been integrated in a transient stability program which applies the simultaneous implicit method of numerical simulation to the network equations stated in the current balance form. The ability of the feedback controller in optimizing the wind production has been concentrated. The DFIG wind turbine active power control is achieved by the convenient control of the rotor voltage. It is significantly the improved performance of the wind turbine system. The proposed method of the feedback controller for the DFIG wind turbine is obtained by the maximum power. The feedback controller is designed for the consideration of both mechanical and electrical dynamics of the DFIG wind turbine. In this paper, system reliability is increased by using a feedback technique. The observer is used to evaluate this information. The results show satisfactory system response and good performance in comparison to the other method. Finally, it is interesting to model the relatively complex energy system scenario analytically to demonstrate the applications of the feedback approach.

Appendix

$$K_1 = \begin{bmatrix} 0.00589 & 0.00489 & 0 & 0 & 0 & 0 \\ 0.0888 & 0.0665 & 0 & 0 & 0 & 0 \end{bmatrix},$$

$$K_2 = \begin{bmatrix} -0.0022 & -0.00315 & -0.0027 & -0.00192 & -0.0012 & -0.0023 \\ -0.0022 & -0.00315 & -0.0027 & -0.0092 & -0.0012 & -0.0023 \end{bmatrix};$$

$$A_{11} = \begin{bmatrix} a_1 & -a_2 & a_3 \\ a_2 & a_1 & a_4 \\ a_7 & a_8 & 0 \end{bmatrix}, \qquad A_{12} = \begin{bmatrix} a_4 & 0 & 0 \\ a_3 & 0 & 0 \\ \omega_s & 0 & 0 \end{bmatrix},$$

$$A_{21} = \begin{bmatrix} -a_8 & a_7 & \omega_s \\ 0 & 0 & 0 \\ 0 & 0 & 0 \end{bmatrix}, \qquad A_{22} = \begin{bmatrix} 0 & 0 & 0 \\ 0 & a_9 & -\omega_s \\ 0 & \omega_s & a_9 \end{bmatrix}.$$

$$B_{11} = \begin{bmatrix} a_5 & 1 \\ a_5 & a_6 \end{bmatrix}, \qquad B_{12} = \begin{bmatrix} 0_{2\times2} \\ 0_{2\times2} \end{bmatrix},$$

$$B_{22} = \begin{bmatrix} 0_{2\times2} \\ 0_{2\times2} \end{bmatrix}, \qquad B_{23} = \begin{bmatrix} a_{10} & -1 \\ a_{10} & a_{11} \end{bmatrix}.$$

$$a_1 = \frac{2}{3}\alpha_1(r_s l_r + r_r l_s), \qquad a_2 = \omega_{slip}, \qquad a_3 = (\alpha_1 r_r V_{ds} + p\alpha_1 l_r V_{ds}\omega_r),$$

$$a_4 = (\alpha_1 r_r V_{qs} + p\alpha 1 l_r V_{qs}\omega_r), \qquad a_5 = \alpha_1 l_m V_{ds},$$

$$a_6 = \alpha_1 l_m V_{ds}, \qquad a_7 = \alpha_3 r_r V_{ds}, \qquad a_8 = \alpha_3 r_r V_{qs},$$

$$a_9 = \frac{r_f}{l_f}, \qquad a_{10} = \frac{3}{2}\frac{V_{ds}}{l_f}, \qquad a_{11} = \frac{3}{2}\frac{V_{qs}}{l_f}.$$

$$c_{11} = \begin{bmatrix} 0 & -\frac{P^2}{JV_s} \\ \frac{P^2}{JV_s} & 0 \end{bmatrix}, \qquad E_{11} = \begin{bmatrix} b_1 & 0 \\ 0 & b_2 \end{bmatrix},$$
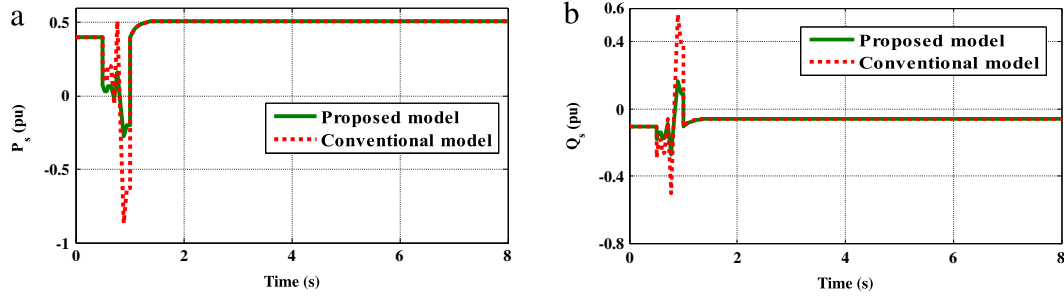
Fig. 8. (a) Performance stator real power versus time, (b) Performance stator reactive power versus time.
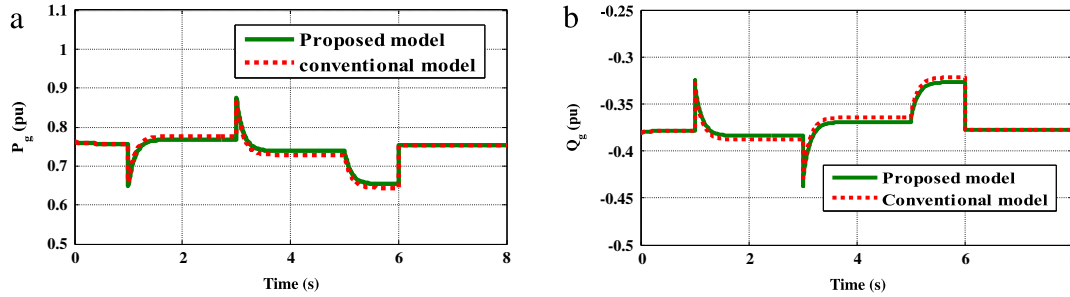

Fig. 9. (a) Performance real power of GSC versus time, (b) Performance reactive power of GSC versus time.

$$E_{21} = \begin{bmatrix} 0 & 0 \\ 0 & 0 \end{bmatrix}, \qquad E_{31} = \begin{bmatrix} b_2 & 0 \\ 0 & b_1 \end{bmatrix}, \qquad E_{22} = \begin{bmatrix} b_3 & 0 \\ 0 & b_4 \end{bmatrix}$$

$$b_1 = \frac{l_s v_{ds}}{l_m |v_s|^2}, \qquad b_2 = \frac{l_s v_{qs}}{l_m |v_s|^2}, \qquad b_3 = 1.5 \frac{\lambda_{ds}}{l_m}, \qquad b_4 = 1.5 \frac{\lambda_{qs}}{l_m}.$$

References

Abdel-Khalik, A., Elserougi, A., Massoud, A., Ahmed, S., 2013. A power control strategy for flywheel doubly-fed induction machine storage system using artificial neural network. Electr. Power Syst. Res. 96, 267–276.

Asl, H.J., Yoon, J., 2016. Power capture optimization of variable-speed wind turbines using an output feedback controller. Renew. Energy 86, 517–525.

Baloch, M.H., Wang, J., Kaloi, G.S., 2016. Stability and nonlinear controller analysis of wind energy conversion system with random wind speed. Int. J. Electr. Power Energy Syst. 79, 75–83.

Balogun, A., Ojo, O., Okafor, F., 2013. Decoupled direct control of natural and power variables of doubly fed induction generator for extended wind speed range using feedback linearization. IEEE J. Emerg. Sel. Top. Power Electron. 1, 226–237.

Baroudi, J.A., Dinavahi, V., Knight, A.M., 2007. A review of power converter topologies for wind generators. Renew. Energy 32, 2369–2385.

Bourdoulis, M.K., Alexandridis, A.T., 2014. Direct power control of DFIG wind systems based on nonlinear modeling and analysis. IEEE J. Emerg. Sel. Top. Power Electron. 2, 764–775.

Carrasco, J.M., Franquelo, L.G., Bialasiewicz, J.T., Galván, E., Guisado, R.C.P., Prats, M.ÁM., et al., 2006. Power-electronic systems for the grid integration of renewable energy sources: A survey. IEEE Trans. Ind. Electron. 53, 1002–1016.

Dinesh, T., Rajasekaran, R., 2015. Independent operation of DFIG-based WECS using resonant feedback compensators under unbalanced grid voltage conditions. In: 2015 International Conference on Innovations in Information, Embedded and Communication Systems (ICIIECS). IEEE, pp. 1–8.

Ebrahimi, F., Khayatiyan, A., Farjah, E., 2016. A novel optimizing power control strategy for centralized wind farm control system. Renew. Energy 86, 399–408.

Gayen, P., Chatterjee, D., Goswami, S., 2015. Stator side active and reactive power control with improved rotor position and speed estimator of a grid connected DFIG (doubly-fed induction generator). Energy 89, 461–472.

Hu, J.-B., He, Y.-K., Wang, H.-S., Lie, X., Coordinated control of grid- and rotor-side converters of doubly-fed induction generator under unbalanced network voltage conditions. In: Zhongguo Dianji Gongcheng Xuebao(Proceedings of the Chinese Society of Electrical Engineering): Chinese Society for Electrical Engineering; 2010. pp. 97–104.

Hu, J., Nian, H., Hu, B., He, Y., Zhu, Z., 2010. Direct active and reactive power regulation of DFIG using sliding-mode control approach. IEEE Trans. Energy Convers. 25.4, 1028–1039.

Junyent-Ferré, A., Gomis-Bellmunt, O., Sumper, A., Sala, M., Mata, M., 2010. Modeling and control of the doubly fed induction generator wind turbine. Simul. Modell. Pract. Theory 18, 1365–1381.

Krause, P.C., Wasynczuk, O., Sudhoff, S.D., Pekarek, S., 2013. Analysis of Electric Machinery and Drive Systems. John Wiley & Sons.

Lei, Y., Mullane, A., Lightbody, G., Yacamini, R., 2006. Modeling of the wind turbine with a doubly fed induction generator for grid integration studies. IEEE Trans. Energy Convers. 21, 257–264.

Luna, A., Lima, F.K.A., Santos, D., Rodríguez, P., Watanabe, E.H., Arnaltes, S., 2011. Simplified modeling of a DFIG for transient studies in wind power applications. IEEE Trans. Ind. Electron. 58, 9–20.

Mishra, Y., Mishra, S., Li, F., Dong, Z.Y., Bansal, R.C., 2009. Small-signal stability analysis of a DFIG-based wind power system under different modes of operation. IEEE Trans. Energy Convers. 24, 972–982.

Naidu, S., Krishna, N., Singh, B., 2014. Sensorless control of single voltage source converter-based doubly fed induction generator for variable speed wind energy conversion system. IET Power Electron. 7, 2996–3006.

Patel, M.R., 2005. Wind and Solar Power Systems: Design, Analysis, and Operation. CRC press.

Rahimi, M., 2016. Drive train dynamics assessment and speed controller design in variable speed wind turbines. Renew. Energy 89, 716–729.

Rezaei, E., Tabesh, A., Ebrahimi, M., 2012. Dynamic model and control of DFIG wind energy systems based on power transfer matrix. IEEE Trans. Power Deliv. 27, 1485–1493.

Tohidi, S., Behnam, M-i., 2016. A comprehensive review of low voltage ride through of doubly fed induction wind generators. Renew. Sustainable Energy Rev. 57, 412–419.

Trilla, L., Bianchi, F.D., Gomis-Bellmunt, O., 2014. Linear parameter-varying control of permanent magnet synchronous generators for wind power systems. IET Power Electron. 7, 692–704.

Wang, L., Wang, K.-H., 2011. Dynamic stability analysis of a DFIG-based offshore wind farm connected to a power grid through an HVDC link. IEEE Trans. Power Syst. 26, 1501–1510.

Xiao, S., Geng, H., Zhou, H., Yang, G., 2013. Analysis of the control limit for rotor-side converter of doubly fed induction generator-based wind energy conversion system under various voltage dips. IET Renew. Power Gener. 7, 71–81.

Yang, L., Xu, Z., Østergaard, J., Dong, Z.Y., Wong, K.P., 2012. Advanced control strategy of DFIG wind turbines for power system fault ride through. IEEE Trans. Power Syst. 27, 713–722.

Yaramasu, V., Wu, B., Sen, P.C., Kouro, S., 2015. Narimani M. High-power wind energy conversion systems: State-of-the-art and emerging technologies. Proc. IEEE 103, 740–788.

Yousefi-Talouki, A., Pouresmaeil, E., Jørgensen, B.N., 2014. Active and reactive power ripple minimization in direct power control of matrix converter-fed DFIG. Int. J. Electr. Power Energy Syst. 63, 600–608.

Zhan, T.-S., Chen, J.L., Chen, S.-J., Huang, C.-H., Lin, C.-H., 2014. Design of a chaos synchronisation-based maximum power tracking controller for a wind-energy-conversion system. IET Renew. Power Gener. 8, 590–597.